Flow and Heat Transfer Measurements Along a Cooled Supersonic Diffuser

Lloyd H. Back,* Robert F. Cuffel,† and Paul F. Massier‡
Jet Propulsion Laboratory, California Institute of Technology, Pasadena, California

An experimental investigation was conducted to ascertain the mean flowfield, including shock wave structure, separated flow regions, turbulent boundary-layer growth, static pressure variations, wall heat transfer, and shear stresses in a second-throat, axisymmetric, supersonic diffuser with wall cooling. The diffuser inlet Mach number of the heated air flow was 3.76, the stagnation pressure was 6.8 atm, the ratio of wall to total gas temperature was 0.44, and the diffuser discharged to the atmosphere. The complex flowfield involved deceleration and acceleration regions, supersonic and embedded subsonic regions, and strong viscous regions with relatively large radial and axial variations. The heat transfer and wall static pressure distributions were remarkably similar, and heat transfer rates were high locally at oblique shock/turbulent boundary-layer interactions, in the pseudoshock region, and in the separation region in the diffuser outlet section.

Nomenclature

D = diffuser throat diameter
h = heat transfer coefficient
H = enthalpy
M = Mach number
P = static pressure
P_t = total (stagnation) pressure
P_t' = pitot pressure
q_w = wall heat flux
r = radial distance
T = static temperature
T_t = total (stagnation) temperature
u = velocity component parallel to wall
u_τ = friction velocity $(\tau_w/\rho_w)^{1/2}$
x = axial distance along the diffuser
y = distance normal to wall
y^+ = dimensionless normal distance $(\rho_w u_\tau y/\mu_w)$
δ = velocity boundary-layer thickness
γ = specific heat ratio
ϵ = expansion area ratio
μ = viscosity
ρ = density
τ_w = wall shear stress

Subscripts

a = atmospheric condition
e = condition at freestream edge of boundary layer
t = stagnation condition
w = wall condition
0 = in duct upstream of nozzle

Introduction

SUPERSONIC diffusers are used during ground-level tests of rocket engines to reduce the back pressure at the supersonic nozzle exit below atmospheric pressure. Sufficient reduction in back pressure allows engine tests to be conducted at chamber pressures without shock-induced flow separation occurring in the divergent section of the nozzle. Numerous investigations have been conducted, including earlier studies of Massier and Roschke,[1,2] which pertain to the influence of configuration on pressure recovery, the usual criterion associated with recovery across a normal shock wave. However, the actual compression process in the diffuser often involves oblique shock waves, a nearly normal shock wave, and a strong compression region that may be shock free but predominantly viscous, which has been referred to as pseudoshock.[3]

Diffuser configurations vary in design for different applications, such as rocket engine testing, wind tunnels, and gasdynamic and chemical laser flows. Diffusers can be attached to or detached from the supersonic nozzle, have smooth or abrupt entrances, incorporate either constant or variable cross-sectional areas associated with converging and diverging sections or centerbodies, and have circular or rectangular cross sections. A predominant feature of diffusers with a contracting or abrupt entrance region is the compressive turning of the flow and the generation of an oblique shock wave that undergoes subsequent reflections from the centerline and the boundary layer along the wall before terminating in the strong compression region.

This investigation is directed toward the second-throat-type diffuser configuration. The axisymmetric diffuser attached smoothly to an axisymmetric nozzle with an expansion area ratio $\epsilon = 9.9$ for which the Mach number of the heated air flow was 3.76 at the diffuser inlet (Fig. 1), and the static to stagnation pressure and temperature ratios were 0.00912 and 0.261, respectively ($\gamma = 1.4$). The entrance section of the diffuser converged to a constant-diameter throat section and then diverged in the short exit section (Fig. 1). Even though in rocket engine tests diffuser inlet Mach numbers are usually greater because of larger nozzle expansion area ratios, the present measurements do extend the range of thermal and flow data in diffusers to higher Mach numbers and consequently to stronger compression processes than previously. Previous wall heat flux and wall static pressure measurements, along with schlieren flow visualization, have been reported by Baker[4] in a square diffuser of constant cross-sectional area into which air at a relatively low Mach number of about 1.5 flowed from a rectangular nozzle. The nozzle spanned the width of the diffuser but was about ¼ the height of the diffuser, so that there was an abrupt expansion at the diffuser inlet. Some recent schlieren, wall static pressure, and pitot tube measurements were made in an airflow through an abrupt entrance supersonic rectangular diffuser with expansion area ratios ϵ from 3 to 15 by Stone,[5] but essentially for adiabatic flow.

Received Feb. 15, 1983; revision received July 21, 1983.

*Group Supervisor.

†Member of the Technical Staff (present address: Walla Walla College, Wash.).

‡Executive Assistant.

Earlier heat transfer and wall pressure measurements were reported in Ref. 6 for the system investigated herein, but with a longer subsonic duct upstream of the nozzle. The system was operated subsequently with a relatively short subsonic duct upstream of the nozzle, and relatively small pitot tube, static pressure probe, and aspirating thermocouple probe surveys were made across the flow at numerous axial locations along the diffuser. These measurements, together with the more detailed heat transfer and wall static pressure distributions obtained, allow a complete picture of the mean flowfield to be constructed, including the shock wave structure, separated flow regions, turbulent boundary-layer growth, static pressure variations, heat transfer, and wall shear stresses in the diffuser as reported herein. Detailed information on the first oblique shock wave/turbulent boundary-layer interaction in the diffuser and on the pseudoshock region was presented in Refs. 7 and 8, respectively. This paper is concerned with the overall thermal and flow behavior for the entire diffuser with wall cooling that has not been reported before. Heat transfer rates are important in determining cooling requirements in diffusers, especially since shock wave/turbulent boundary-layer interactions and pseudoshock regions cause higher heating rates than when such phenomena are not present.

Experimental Apparatus and Measurements

The cooled system consisted of a short subsonic duct (12.7 cm in diameter and 1.4 diameters long), a supersonic nozzle

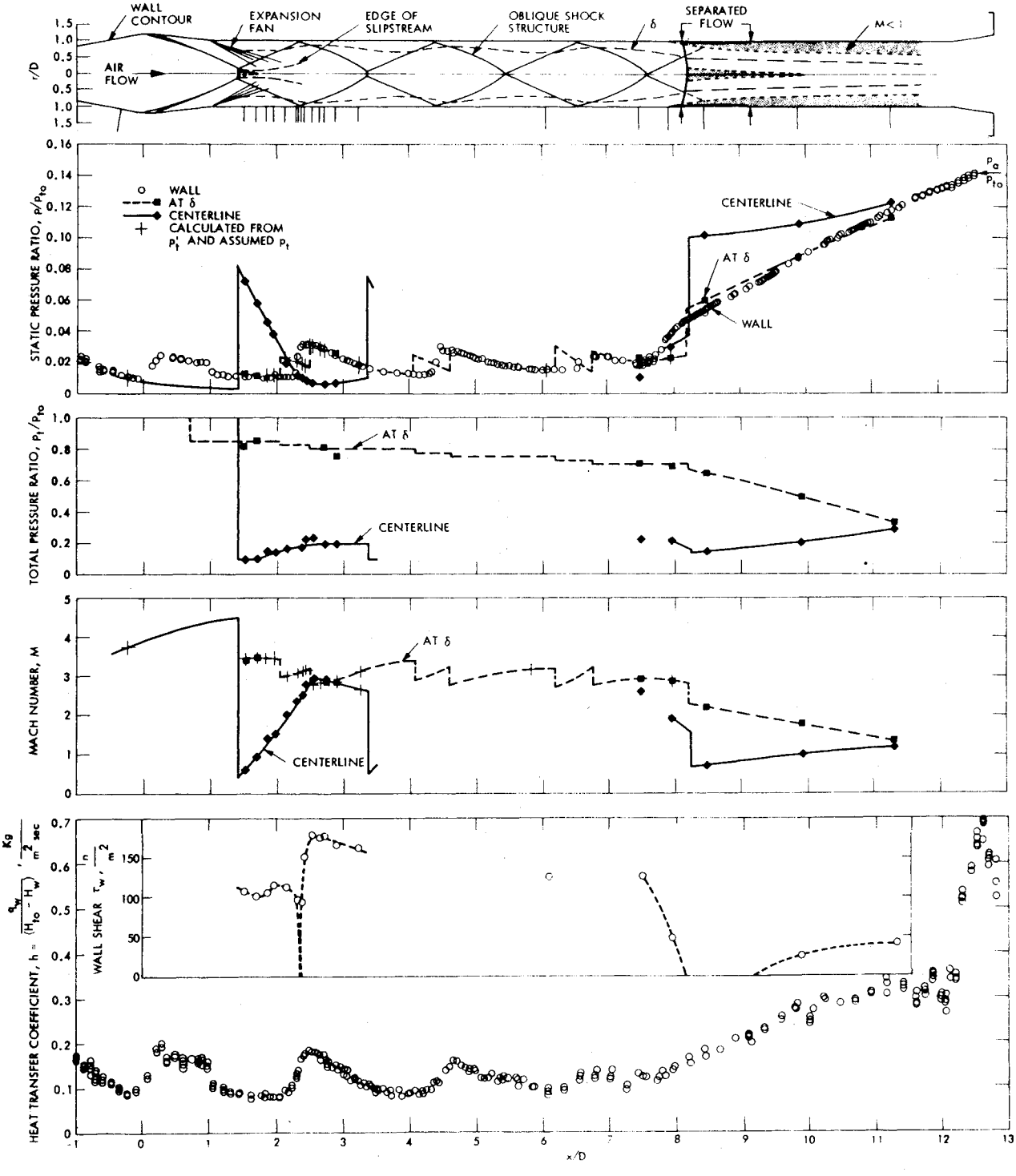

Fig. 1 Diffuser flowfield and measurements along the wall, edge of the boundary layer δ, and along the centerline of the diffuser.

(with convergent and divergent half-angles of 10 deg and a circular-arc throat region with a 4.04-cm-diam throat and 12.70-cm exit diameter), and the diffuser. The diffuser, which is shown in Fig. 1 along with the downstream part of the nozzle divergent section, had a second-throat diameter of 10.8 cm. The diffuser was 11 second-throat diameters long and had short inlet and outlet sections with 6 and 8 deg half-angles, respectively.

Ambient air was compressed and heated at a remote distance upstream, and was accelerated to a nearly uniform flow at the subsonic duct inlet with a thin, tripped velocity boundary layer that was determined to be turbulent. The air mass flow rate was measured with an orifice prior to heating by the internal combustion of methanol. The flow rate of methanol was measured with a rotameter. The total gas flow rate of the products of combustion was 1.18 kg/s. Thermodynamic properties and flow variables were calculated for the products of combustion with $\gamma = 1.4$, but transport properties were calculated for air since the methanol-to-air mass flow was only 3.1%. The flow discharged from the diffuser into the ambient air.

The diffuser started at a stagnation pressure of 5.51 atm, which was slightly below the starting pressure of 5.63 atm computed using normal shock theory at the diffuser inlet. There was negligible hysteresis, i.e., the minimum starting pressure was the same as the minimum operating pressure. The stagnation pressure P_{t0}, measured with a pitot tube along the centerline just upstream of the nozzle in the cooled duct section, was 6.83 atm for most of the data presented. The data in the pseudoshock region were obtained at a slightly lower stagnation pressure of 6.55 atm. The data along the upstream portion of the diffuser were relatively insensitive to the stagnation pressure within the small variations in the tests. The ambient pressure was 0.959 atm.

The stagnation temperature T_{t0} of the gas flow measured just upstream of the nozzle in the cooled duct section by three thermocouples spaced 90 deg apart circumferentially at the pitot tube location was 838 K. The entire cooled system was instrumented with individual, circumferential coolant passages and wall static pressure taps. The warm water circulated in the coolant passages maintained the wall to total gas temperature ratio T_w/T_{t0} near 0.44. The wall heat flux for each circumferential passage was obtained by calorimetry, and semilocal heat transfer coefficients were computed from

$$h = \frac{q_w}{(H_{t0} - H_w)}$$

The gas side-wall temperature and thus enthalpy H_w were determined from the heat flux measurements and thermocouple measurements on the inside wall of the coolant passages via the heat conduction equation. The wall static pressure distribution along the diffuser was determined from numerous sharp-edged 0.051-cm-diam taps. Differences between wall static pressure and atmospheric pressure were measured with transducers.

Pitot, static pressure, and aspirating thermocouple probes were traversed across the flow just upstream and along the diffuser at numerous stations indicated by the vertical lines drawn below the diffuser as shown in Fig. 1. A short distance upstream of the diffuser inlet, at $x/D = -0.33$, where the Mach number was 3.51, the boundary layer was turbulent with momentum thickness $\theta = 0.080$ cm, displacement thickness $\delta^* = 0.061$ cm, energy thickness $\phi = 0.21$ cm, estimated boundary-layer thickness $\delta \simeq 1.4$ cm, and momentum thickness Reynolds number $\rho_e u_e \theta/\mu_e = 6.670$. The wall shear stress was estimated from the boundary-layer measurements with the relatively small tip probes that extended into the viscous sublayer (y^+ on the order of 10). Local flow separation regions were detected by bleeding a small amount of ammonia gas through the wall static pressure tap holes and observing the streak patterns in a thin film of ammonia-sensitive ozalid paint on the surface. Further information on the probe measurement technique, including probe size, accuracy of the probe measurements, and consistency with the wall measurements, was presented in Refs. 7 and 8, along with radial distributions of velocity, mass flux, and total temperature, and is not repeated herein.

Results

The overall aspects of the flow are seen in Fig. 1 where data are shown along the wall, at the edge of the boundary layer δ, and along the centerline of the diffuser. The flow structure including shock waves and separated flow regions as determined from the probe and wall measurements is depicted in the diffuser in Fig. 1. The oblique shock wave system was generated in the wall region at the nozzle exit where the flow was turned to flow into the diffuser inlet. This shock wave was reflected from the centerline through a shock stem (Mach reflection) and then was incident on the boundary layer at the first wall interaction. The detailed shock wave/boundary-layer interaction results in Ref. 7 indicated that this incident shock wave penetrated deeply into the outer supersonic part of the turbulent boundary layer and produced a very small separation region of length and height 0.46 and 0.01 cm, respectively (not observable in the scale of Fig. 1). The separation shock (formed by the coalescing of compression waves associated with separation) merged with the reflected shock (generated by the compressive turning of the flow back again to follow along the wall) at the outer edge of the boundary layer downstream of impingement. This reflected shock wave underwent subsequent centerline and boundary-layer reflections before terminating in the region of a strong Mach-disk-like shock wave, which was normal to the flow at the centerline, and was associated with compressive turning of the flow radially inward beyond the separated flow region depicted in Fig. 1. The boundary layer reattached downstream. The size of this separation region was considerably larger than at the upstream oblique shock wave/boundary-layer interaction, being one diffuser diameter in length, but relatively thin—about 4% of the diffuser radius r_w. An expansion fan emanating at the corner of the intersection of the diffuser inlet and throat sections associated with the 6 deg turning and the viscous slipstream region downstream of the centerline Mach reflection are also aspects of the diffuser flow (Fig. 1). Information on the latter was presented in Ref. 9 for unheated air flow.

The flowfield in the diffuser was very complex, involving deceleration and acceleration regions, supersonic and subsonic regions, and strong viscous regions with relatively large radial and axial variations. Flow deceleration and compression occurred across the oblique shock waves, while the flow between the oblique shock waves accelerated and expanded to maintain the mass balance for the diffuser flow. Turbulent boundary-layer growth in the oblique shock wave region was strongly influenced by the shock wave interactions that caused the boundary layer to become thinner as a result of the turning of the flow toward the wall by the incident shock. Between the incident shock waves the supersonic boundary layer thickened in the acceleration regions. The net effect of this thinning and thickening process was to barely change the boundary-layer thickness upstream of the Mach-disk-like shock wave from that at the diffuser throat inlet. There was considerable boundary-layer growth in the region of the Mach-disk-like shock wave because of the radially inward turning of the flow and separation. Downstream of the Mach-disk-like shock wave the thick subsonic portion of the boundary layer formed in the separation process grew as the flow progressed downstream. The flow accelerated in regions along the wall[8] and near the centerline, with the latter resulting in supersonic flow again. However, the bulk of the flow located in an annular region between these two accelerating flow regions decelerated,[8] which is associated with

the strong compression process as the static pressure increase along the centerline extended toward the wall, and the boundary layer grew in thickness.

There were large differences between total pressures along the centerline and at the edge of the boundary layer, primarily because of the shock waves (as depicted in Fig. 1). Total pressure changes across locally normal shock waves decreased as the local upstream Mach numbers diminished (Fig. 1); and obviously there were smaller total pressure changes across the oblique shock waves at the edge of the boundary layer. The flow along the centerline at the nozzle exit continued to expand in the diffuser to a higher Mach number, with the consequent total pressure loss across the centerline Mach reflection principally setting the total pressure level along the centerline of the diffuser. In the viscous pseudoshock region, the higher total pressures at the edge of the boundary layer upstream in the oblique shock region decreased more rapidly and merged with the rising total pressures along the centerline.

The wall static pressure increased across the shock wave generated at the diffuser inlet and then decreased at the corner at the diffuser throat inlet before undergoing subsequent increases at oblique shock wave/boundary-layer interactions and decreases in the expansion regions between the interactions indicated in Fig. 1. At the edge of the boundary layer, the discrete pressure rises across the incident and reflected shock waves are noted, as is the variation along the centerline associated with the Mach reflections. The net effect of the oblique shock wave/boundary-layer interactions is to increase the wall static pressure just upstream of the Mach-disk-like shock wave above the value at the diffuser inlet. In the pseudoshock region the major pressure rise occurred, with propagation of the increased pressure radially outward toward the wall in the flow direction.

The variation of the heat transfer coefficient along the diffuser (Fig. 1) is remarkably similar to the wall static pressure variation, increasing at oblique shock wave/boundary-layer interactions, and decreasing at the inlet corner region and between the interactions. This correspondence is believed to be primarily the result of the relationship between mass flux ρu and pressure for supersonic flow, i.e., mass fluxes increase with increasing pressures and vice versa; although the analysis presented in Ref. 10 has indicated a weaker dependence on static temperature change as well as the mass flux change across compressive interactions. In the pseudoshock region, as in the oblique shock wave/boundary-layer interactions, the relationship between the heat transfer coefficient and wall static pressure was given by $h \alpha P_w^{0.8}$, except in the short diffuser outlet section where flow separation is believed to have occurred in the thickened subsonic boundary layer because of the 8 deg corner half-angle, and where an appreciable increase in the heat transfer coefficient was measured.

At the first oblique shock wave/boundary-layer interaction the wall shear stress increased across the interaction, whereas in the pseudoshock region it also increased again in the reattached region, but remained below the upstream value (Fig. 1). Values of the wall shear stress less than zero correspond to the separated flow regions. The magnitude of the increase in the wall shear stress at the oblique shock wave/boundary-layer interaction can be estimated as indicated in Ref. 7.

Conclusions

The present measurements have indicated the complex flow structure and heat transfer in a second-throat supersonic diffuser with wall cooling. The flow considered exhibited various regimes that have not been described adequately, if at all, by theoretical analyses. Clearly, more work is needed to acquire a better understanding of the interrelationships between supersonic flow phenomena and viscous interactions in turbulent duct flows that would lead to fundamental prediction methods for the location and structure of the shock wave system, boundary-layer growth, and wall heat transfer as a function of pressure ratio and diffuser configuration.

References

[1]Massier, P. F. and Roschke, E. J., "Experimental Investigation of Exhaust Diffusers for Rocket Engines," *Progress in Astronautics and Rocketry: Liquid Rockets and Propellants,* Vol. 2, Academic Press, New York, 1960, pp. 3-75.

[2]Massier, P. F. and Roschke, E. J., "Application of Exhaust Diffusers for Rocket Engine Testing," Jet Propulsion Laboratory, Pasadena, Calif., TM 33-97, Aug. 1962.

[3]Crocco, L., "One-Dimensional Treatment of Steady Gas Dynamics," *Fundamentals of Gas Dynamics*, Vol. III, edited by H. W. Emmons, Princeton University Press, Princeton, N.J., 1958, p. 115.

[4]Baker, P. J., "Heat Transfer in a Supersonic Parallel Diffuser," *Journal of Mechanical Engineering Science*, Vol. 7, No. 1, 1965, pp. 1-7.

[5]Stone, W. C., "Analytical and Experimental Characterization of a 2-D Supersonic Diffuser with Abrupt Entrance Geometry," Ph.D. Dissertation, University of Alabama, Huntsville, Ala., Dec. 1982.

[6]Back, L. H., Cuffel, R. F., and Massier, P. F., "Experimental Convective Heat Transfer and Pressure Distributions and Boundary Layer Thicknesses in Turbulent Flow Through a Variable Cross-Sectional Area Channel," *4th International Heat Transfer Conference*, Paris-Versailles, Vol. II, FC 2.1, 1970, pp. 1-14.

[7]Back, L. H. and Cuffel, R. F., "Shock Wave-Turbulent Boundary Layer Interactions With and Without Surface Cooling," *AIAA Journal*, Vol. 14, April 1976, pp. 526-532.

[8]Cuffel, R. F. and Back, L. H., "Flow and Heat Transfer Measurements in a Pseudo-Shock Region with Surface Cooling," *AIAA Journal*, Vol. 14, Dec. 1976, pp. 1716-1722.

[9]Back, L. H. and Cuffel, R. F., "Viscous Slipstream Flow Downstream of a Centerline Mach Reflection," *AIAA Journal*, Vol. 9, Oct. 1971, pp. 2107-2109.

[10]Back, L. H. and Cuffel, R. F., "Changes in Heat Transfer from Turbulent Boundary Layers Interacting with Shock Waves and Expansion Waves," *AIAA Journal*, Vol. 8, Oct. 1970, pp. 1871-1873.